Capillary passive valve in microfluidic systems

Hansang Cho*, Ho-Young Kim†, Ji Yoon Kang*, and Tae Song Kim*

*Microsystem Research Center, †Thermal/Flow Control Research Center
Korea Institute of Science and Technology, Seoul 136-791, Korea
Tel: 82-2-958-6708; Fax : 82-2-958-6910; E-mail: hscho@kist.re.kr

ABSTRACT

This work reports the theoretical and experimental investigations of capillary bust valves to regulate liquid flow in microchannels. The theoretical analysis uses the Young-Laplace equation and geometrical considerations to predict the pressure at the edge of the valve opening. Numerical simulations are employed to predict the meniscus shape evolution while the interface is pinned at the valve edge. Microchannel and valves are fabricated using the soft lithography. A wafer-rotating system, which can adjust a driving pressure by rotational speed, induces a liquid flow. Experimentally measured valve-bursting pressure agrees with theoretical predictions.

Keywords: capillary burst valve, microfluidcs, soft lithography, microchannel

1 INTRODUCTION

In microfluidic systems, valves are essential components to control the sequence of bio/chemical analyses. Among various valve schemes proposed to date [1, 2], a capillary passive valve is especially attractive because it is insensitive to physicochemical properties of the liquid and easy to fabricate by rapid prototyping. [2, 3] Although its basic concepts have been empirically verified before [2], its physical understanding is still far from complete. Recently delicate body forces generated in rotational motion are studied to drive microfluid. [1, 2, 4] This work rigorously analyzes the hydrodynamics of the capillary passive valve for the first time. Numerical simulations are conducted to predict meniscus shape evolution while the interface is pinned. Furthermore, the microfluidic valve and rotational wafer system is fabricated and driven by centrifugal force and its operation is visualized by a triggered video system.

2 THEORETICAL ANALYSIS

2.1 Pressure Difference across the Liquid Meniscus

The pressure difference across the liquid meniscus, ΔP_S is given by the Young-Laplace equation:

$$\Delta P_S = P_i - P_o = \sigma\left(1/R_1 + 1/R_2\right) \tag{1}$$

where P_i and P_o respectively denote the pressure inside and outside the liquid interface, and R_1 and R_2 are the principal radii of curvature. In a liquid channel, the radii of curvature are determined by the dimensions of the channel and the contact angle. Geometric considerations yield the following relation for the pressure difference in a straight channel:

$$\Delta P_S = -2\sigma\cos\theta_A\left(1/h + 1/w\right) \tag{2}$$

where σ is the surface tension, θ_A is the advancing contact angle, and w and h denote the width and the height of the channel, respectively. Here we assume that the advancing contact angle is determined by the liquid/solid combination and fairly insensitive to the speed of contact line. To drive liquid flow inside a hydrophobic microchannel, where ΔP_S positive, external pressure is should be applied to overcome such static pressure barrier and also viscous dissipation related to the liquid velocity.

A liquid flow through a microchannel can be regulated by devising an abruptly widening cross-section in the channel as shown in Fig. 1 (a). This area is called a capillary burst valve. The valve stops a liquid flow by pinning the contact line at the valve edge. The pinning takes place since the contact angle should increase until its value with respect to the new surface reaches the critical advancing angle. Then the pressure profile can be obtained by using a foregoing geometric considerations and the Young-Laplace relation. The analysis shows that the pressure difference occurring at the pinned state is

$$\Delta P_S = -2\sigma\left(\cos\theta_A/h + \cos\theta_I/w\right) \tag{3}$$

where θ_I is the intermediate contact angle which varies from θ_A to $\theta_A + \beta$ as the liquid meniscus bends toward the open area. Here β is the diverging angle of the valve with respect to the straight channel as indicated in Fig. 1 (a). When the driving pressure exceeds the value of Eq. (3), the valve bursts and the static analysis gives the following relation for ΔP_S :

$$\Delta P_S = -2\sigma\left[\cos\theta_A / h + \cos(\theta_A + \beta)/2b\right] \quad (4)$$

Fig. 2 plots ΔP_S as the interface advances through the capillary burst valve, using Eqs. (2-4).

2.2 Pressure Difference in a Rotating System

In this work, we employ a rotating system to drive liquid flow. The driving pressure by a centrifugal force exerted on the liquid in a channel is written as

$$\Delta P_C = \frac{1}{2}\rho\omega^2(r_1^2 - r_2^2) \quad (5)$$

where ρ is the liquid density, ω the constant angular velocity, and r_1 and r_2 are the radius as indicated in Fig. 2.

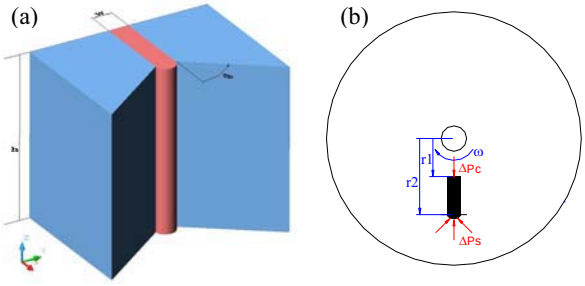

Fig. 1 (a) A schematic of a rectangular channel with a capillary burst valve. (b) Centrifugal force on a liquid in microchannel.

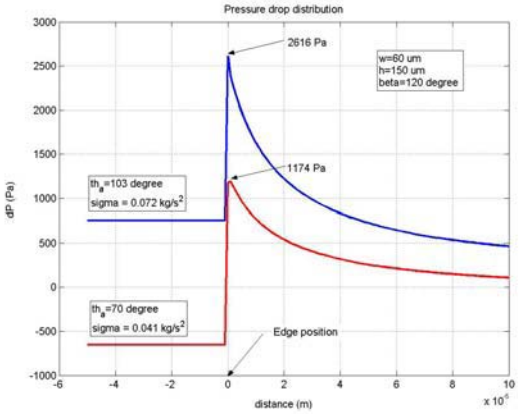

Fig. 2 Pressure difference across the liquid meniscus.

3 NUMERICAL SIMULATIONS

To investigate the temporal evolution of liquid interface at the valve area, a numerical analysis was performed for two-dimensional channels. The channels were composed of two straight lines, which met abruptly diverging area of the valve. Numerical simulations were conducted using commercial software, CoventorWare™. The conditions of the simulations are summarized in Table 1. The simulation results, i.e. the temporal profiles of the advancing interface, are shown in Fig. 3, 4. The figure reveals that the meniscus shapes and wetting are different depending on the value of θ_A and β.

Table 1. Simulation conditions

θ_A		σ	ρ
120°	60°	7.2e-2 kg/s^2	998 kg/m^3

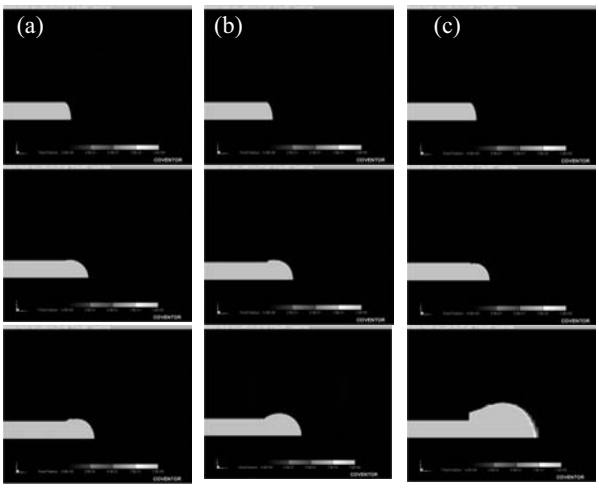

Fig. 3. Evolution of the interface near bursting for hydrophobic case. (a) $\beta = 30^\circ$ (b) $\beta = 60^\circ$ (c) $\beta = 90^\circ$

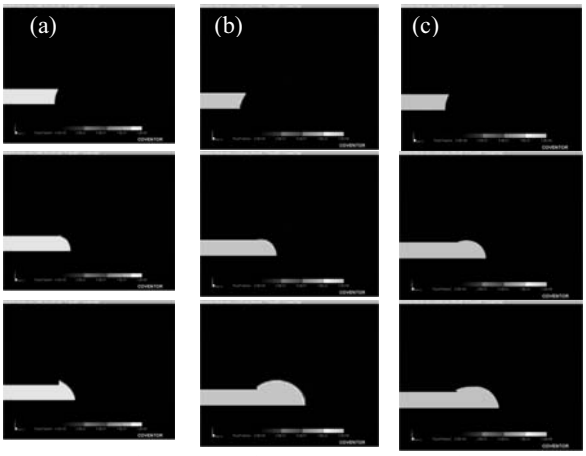

Fig. 4. Evolution of the interface near bursting for hydrophilic case. (a) $\beta = 90^\circ$ (b) $\beta = 120^\circ$ (c) $\beta = 150^\circ$

4 EXPERIMENTAL STUDY

4.1 Design of Valves

The valve stops the liquid flow when the maximum value of ΔP_S given by Eq. (3) exceeds the driving pressure of ΔP_C given by Eq. (5). Therefore, the performance of the valve is determined by h, w, θ_A and β. The bursting pressure can be experimentally investigated by changing the rotational speed for a given liquid. The dimensions of the valves designed for this work are listed in Table 2.

Table 2. Dimensions of the valves used in this work

h	w	β		
150 μm	60 μm	60°	90°	120°

4.2 Fabrication Processes

The channels were fabricated by plastic molding process to decrease time and cost of fabrication. The mother mold was made of a photoresistor (SU-8). The photoresistor was spin-coated with the thickness of 150 µm and patterned using a conventional photolithography technique. A care was taken in baking processes to prevent the photoresitor from undergoing rapid temperature difference for minimizing thermal stress. The thermal stress tends to be concentrated at the opening edge of the valve, eventually deforming the microstructure. The opening edge of the valve was observed with a scanning electron microscope (S4200, Hitachi) to make sure no thermal stress deformation had occurred. The results were compared in fig. 5.

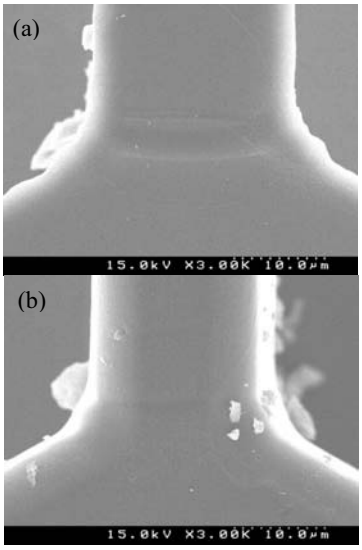

Fig. 5. Edge shape of SU-8 mold. (a) Normal heat treatment. (b) Careful heat treatment.

PDMS was then cast against the mold to yield an electrometric replica. The replication process is illustrated in Fig. 6 (a). The PDMS replica was bonded to a PC (polycarbonate) substrate. For the bonding, the substrate was coated with 1 µm thick Primer 1200 (Dow Corning), which was then cured for 1 hour at room temperature. On the coating, a low-viscosity PDMS solution was spin-coated to a thickness of 10 µm. The replica and the coated substrate were bonded by curing the PDMS coating for 1 hour at 80ºC. Such a process is shown in Fig. 6 (b). The image of the processed wafer is shown in Fig. 7.

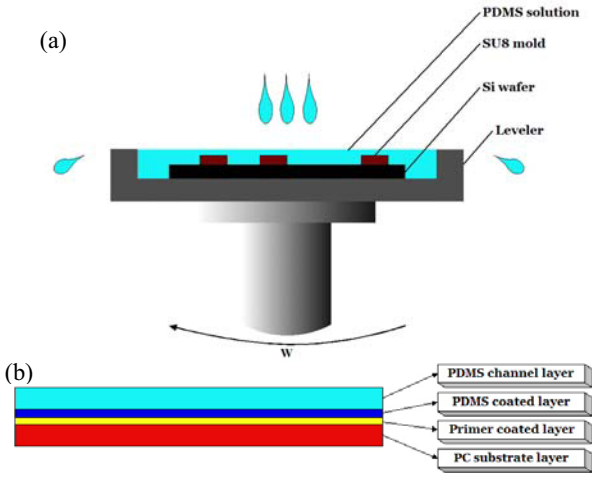

Fig. 6. Fabrication processes for (a) PDMS replica and (b) Wafer layers

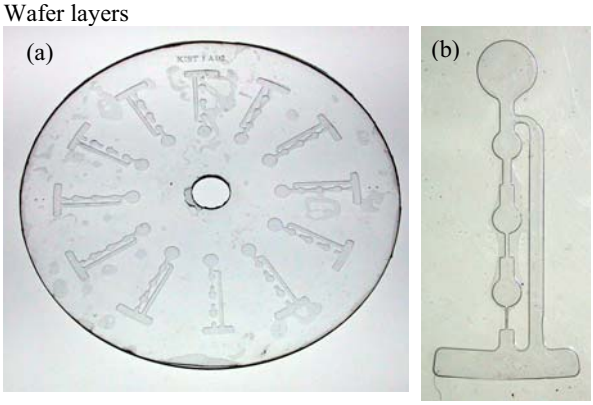

Fig. 7. Images of the processed wafer. (a) The whole wafer. (b) Magnified section.

4.3 Experimental Procedure

The experimental apparatus is shown in Fig. 8. The system rotates a wafer with an AC servo motor controlled by an A/D converter, whose rotational speed ranges between 10 and 10,000 rpm. A CCD (charge coupled device) camera images the rotating wafer in situ using a trigger signal synchronized with a counter connected to a frame grabber. The frame rate ranges between 15 and 30 frames per second and the exposure time can be reduced to 1.25 µs.

A liquid used here is a water-dye (Phenol Red) mixture having physical properties as listed in Table 3. The

microchannel wafer was loaded with the liquid of the volume of about 50 µl. The sample chamber was completely filled with 20 µl of the liquid, and the surplus was bypassed into a waste channel. By rotating the wafer, the liquid filling the sample chamber was driven to flow through a channel. At low rotating speeds, the flow was stopped at the valve. However, by gradually increasing the rotating speed, a critical pressure difference that caused the valve to burst was obtained.

Table 3. Physical properties of the liquid

θ_A	σ	ρ
95°	0.058 kg/s^2	1018.5 kg/m^3

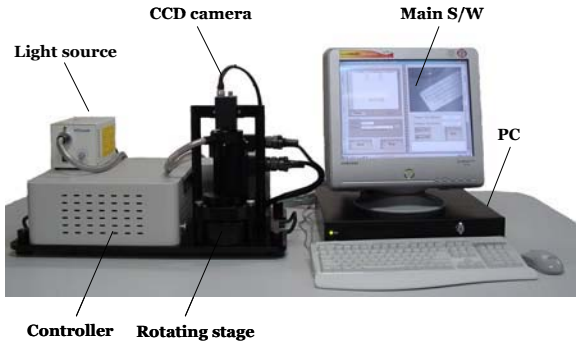

Fig. 8. A schematic of the centrifugal microfluidic system

4.4 Experimental Results

Experimental images of liquid flow around the valve are shown in Fig. 9. The images appear similar to the results obtained by the numerical simulations as discussed above. To compare the experimental measurements of the bursting pressure with our theoretical predictions, tests were performed using valves with different diverging angles, β. Fig. 10 reveals that the experimental results and the theoretical predictions are in a good agreement.

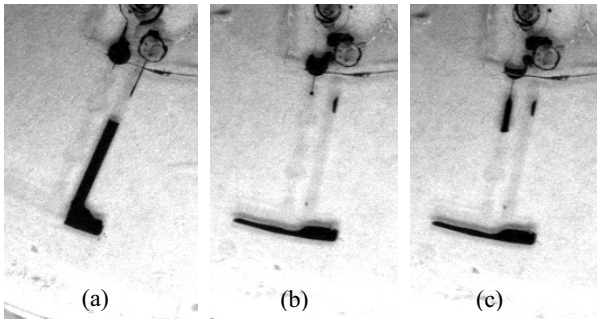

Fig. 9. Experimental images of the liquid around the valve. (a) Before pinning (b) Pinned state (c) After bursting

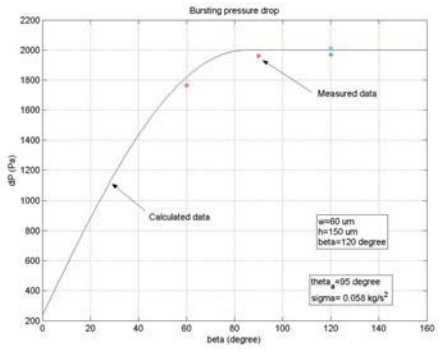

Fig. 10. Theoretical prediction of bursting pressure and experimental measurements.

5 CONCLUSIONS

Capillary burst valves provide attractive means to regulate microscale liquid channel flows since they involve no moving parts and are easy to fabricate. Especially, a wafer-rotation system can easily achieve flow regulation by adjusting rotation speed according to the critical bursting pressure of the valve. This work investigated the pressure difference that the capillary bust valve can withstand depending on the liquid properties and channel dimensions. We provided a rigorous theoretical formulation that predicts the pressure difference developing around the liquid meniscus. Numerical simulations were performed to show the meniscus shape evolution while the interface was pinned. Furthermore, the microfluidic valve and rotational wafer system were fabricated to test the performance of the capillary bust valves. The valve operation was visualized by a triggered video system. The experiments showed that the measurement results and the theoretical predictions were in a good agreement.

Acknowledgments

This research, under the contract project code MS-03-211-01, has been supported by the Intelligent Microsystem Center (IMC; http://www.microsystem.re.kr), which carries out one of the 21st century's Frontier R&D Projects sponsored by the Korea Ministry Of Science & Technology.

REFERENCES

[1] M. J. Madou, C.-H. Shih, *Biomed. Microdevices*, Vol.3, pp. 245~254, 2001

[2] D. C. Duffy, G. J. Kellogg**,** *Anal. Chem.,* Vol.71, pp. 4669 - 4678, 1999

[3] B.-H. Jo, D. J. Beebe*, J MEMS*, Vol.9, pp.76-81, 2000

[4] J. Ducree, R. Zengerle, *µTAS 2003*, pp. 606-606, 2003